Physica B 404 (2009) 4344–4348

Contents lists available at ScienceDirect

Physica B

journal homepage: www.elsevier.com/locate/physb

Shallow levels in virgin hydrothermally grown n-type ZnO studied by thermal admittance spectroscopy

R. Schifano [a], E.V. Monakhov [a], B.G. Svensson [a,*], W. Mtangi [b], P. Janse van Rensburg [b], F.D. Auret [b]

[a] Department of Physics/Center for Materials Science and Nanotechnology, University of Oslo, P.O. Box 1048 Blindern, N-0316 Oslo, Norway
[b] Department of Physics, University of Pretoria, Pretoria 0002, South Africa

ARTICLE INFO

PACS:
61.72.J–
61.72.S–
61.72.uj
71.55.Gs

Keywords:
ZnO
Thermal admittance spectroscopy
Negative-U

ABSTRACT

Three n-type single crystal hydrothermally grown ZnO samples with resistivities of 5.1 ± 0.6, 15 ± 2 and $220 \pm 20\,\Omega$ cm, respectively, have been electrically characterized using thermal admittance spectroscopy (*TAS*). The presence of three main donors: two shallow ones D_1 and D_2 and a deeper one D_3 with activation energies of ~30, ~50 and ~290 meV, respectively, are detected. In addition, the *TAS* spectra reveal the presence of a fourth level, D_X, with a peak amplitude in the conductance spectra that decreases with the temperature occurrence. It is shown that this anomalous behavior is consistent with D_X being a negative-U defect of donor-type. An activation energy of ~80 meV for the ++/+ transition, a capture cross section equal to $\sim 3 \times 10^{-17}$ cm^2 and an energy barrier for atomic reconfiguration of ~0.25 eV, respectively, deduced according to the assignment of D_X to a negative-U defect. A tentative assignment of the D_X defect with oxygen vacancies is discussed.

1. Introduction

The advances in growth of ZnO high quality large-area single crystals [1–3] and the recent reports of p-type conduction [4] are fuelling the renewed interest in this material with potential applications that range from solid state ultraviolet (UV) emitters, to be used as high efficiency lighting devices for general illumination, to high density optical information storage systems, transparent and flexible electronics [5–8]. In addition, from a technological point of view the availability of a inherently scalable technique, like the hydrothermal method, is particularly important for the growth of large-area single crystal ZnO wafers of device-worthy quality [9].

However, substantially improved electrical characterization of ZnO is necessary for a better understanding and exploitation of the material. The limited progress is mainly due to the difficulties [10] in achieving stable and good quality Schottky contacts (*SCs*) that are fundamental for studying defects in semiconductors by junction spectroscopic techniques like admittance spectroscopy (*AS*) and deep-level transient spectroscopy (*DLTS*). Hence, deep level defects in ZnO are poorly understood. For instance, in the ~100–140 meV range below the conduction band edge (E_C) at least two defects levels are, generally, reported to occur [11–15]; one of them is presumably donor related [11,13,16], and associated with the oxygen sublattice [14–18], while, the nature of the other one is almost completely unknown and has been tentatively ascribed to a metastable defect [13]. Furthermore, discrepancies between the main donor position determined by temperature dependent Hall effect measurement (*TDH*) and *DLTS* are found and attributed to a temperature activated capture cross section of the donor like level in the ~100–140 meV range [11].

In this work, thermal admittance spectroscopy (*TAS*) measurements have been performed on hydrothermally grown and nominally undoped n-type ZnO samples. Four distinct energy levels are revealed where one shows an anomalous dependence of the conductance peak height on the temperature of occurrence. *TDH* measurements performed on the same samples unveil only the three well-behaved energy levels, while the anomalous one is not detected. These three levels are all shown to be of donor-type, two having very shallow positions and the third one being substantially deeper. On the other hand, the energy level showing the anomalous behavior is tentatively attributed a +/++ transition of a negative-U center, such as the oxygen vacancy (V_O).

2. Experimental details

Three hydrothermally grown ZnO square samples A, B and C were cut from three different nominally undoped n-type wafers with a resistivity of 5.1 ± 0.6, 15 ± 2 and $220 \pm 20\,\Omega$ cm, respectively, as determined by four point probe measurements. The samples were cleaned in a ultrasonic bath with acetone and ethanol and then dipped in a H_2O_2 solution for 15 min. Finally,

* Corresponding author.
E-mail addresses: ramon.schifano@smn.uio.no (R. Schifano). b.g.svensson@fys.uio.no (B.G. Svensson).

0921-4526/$ - see front matter © 2009 Elsevier B.V. All rights reserved.
doi:10.1016/j.physb.2009.09.030

circular Pd *SC*s were deposited on the O face $(000\bar{1})$ ex situ, at a base pressure of 10^{-6} mbar, via e-beam evaporation from a 99.999% pure metal source through a molybdenum shadow mask, and subsequently, annealed at 200 °C for 30 min in air. The contacts had diameters of 0.26, 0.46 and 0.75 mm with an overall error of 0.01 mm and a nominal thickness of ~100 nm according to quartz-crystal deposition rate monitor.

The *TAS* measurements were undertaken in the 20–330 K temperature range using an Agilent 4284A LCR meter and a closed cycle helium cryostat. The measurements were performed with a test signal of 30 mV at probing frequencies (f_T) of 1, 4, 16, 60, and 250 kHz during sample cool down.

In all cases, an eutectic InGa drop, placed on the sample back side, was used as ohmic contact.

3. Results

3.1. D_1, D_2 and D_3 levels

Typical *TAS* spectra for samples A, B and C at a reverse bias of −1 V are shown in Fig. 1(a), where G is the conductance and f_T the probing frequency. For sample A several overlapping peaks occur in the 50–150 K region. Hence, a detailed analysis is not readily performed, except for the first peak D_1. Anyhow, even for D_1, as can be seen in Fig. 1(b), the deconvolution procedure to determine the peak temperature position is accompanied with a large uncertainty. Furthermore, as shown in Fig. 1(a) G/f_T spectra taken on different *SC*s reveal a variation of the peak amplitudes thus indicating sample inhomogeneities mainly arising from a non-uniform distribution of compensating Li-impurities, as dis cussed in Ref. [19].

The activation energies, E_d, for the defects related to the freeze out peaks (D_1 for sample A, D_2 for sample B and D_3 for sample C) are obtained from the relation [20]:

$$\frac{f_T}{\mu(T)\cdot T_{\max}^{3/2}} \propto \exp\left(\frac{-E_d}{k_B T_{\max}}\right) \quad (1)$$

where k_B is the Boltzmann constant, $T_{\max}$ the temperature at which the conductance peak is occurring and μ is the mobility. For determining the temperature dependence of the right hand side of Eq. (1) a mobility temperature dependence of the kind $\mu_0 T^b$ is assumed. Moreover, the exponent b has been chosen according to the dominant scattering mechanism in the temperature range where freezing out occurs, i.e. $b=1.5$ for D_1 and D_2 and $b=0$ for D_3 [19,21].

For the conductance peaks occurring at temperatures above the freezing out, E_d is extracted according to the standard equation [20,21]:

$$\frac{2\pi\cdot f_T}{T_{\max}^2} \propto \exp\left(\frac{-E_d}{k_B T_{\max}}\right) \quad (2)$$

The resulting activation energies obtained from the Arrhenius plots shown in Fig. 1(b) are summarized in Table 1. The positions of D_1, D_2 and D_3 are also supported from the fitting of *TDH* data, as described elsewhere [19]. Here, it should be pointed out that D_1 is only observed in sample A, which exhibits less compensation, but exists presumably in all the three samples. However, because of strong compensation in sample B and C, D_1 is not detected and a similar conclusion holds for D_2 in sample C.

The activation energies of ~30 meV for D_1 and ~50 meV for D_2 are in agreement with the values expected for H and Al impurities, respectively, and, in case of D_2, the assignment is supported by secondary ion mass spectrometry measurements performed on the same samples [19]. The position of D_3 is in the range of the

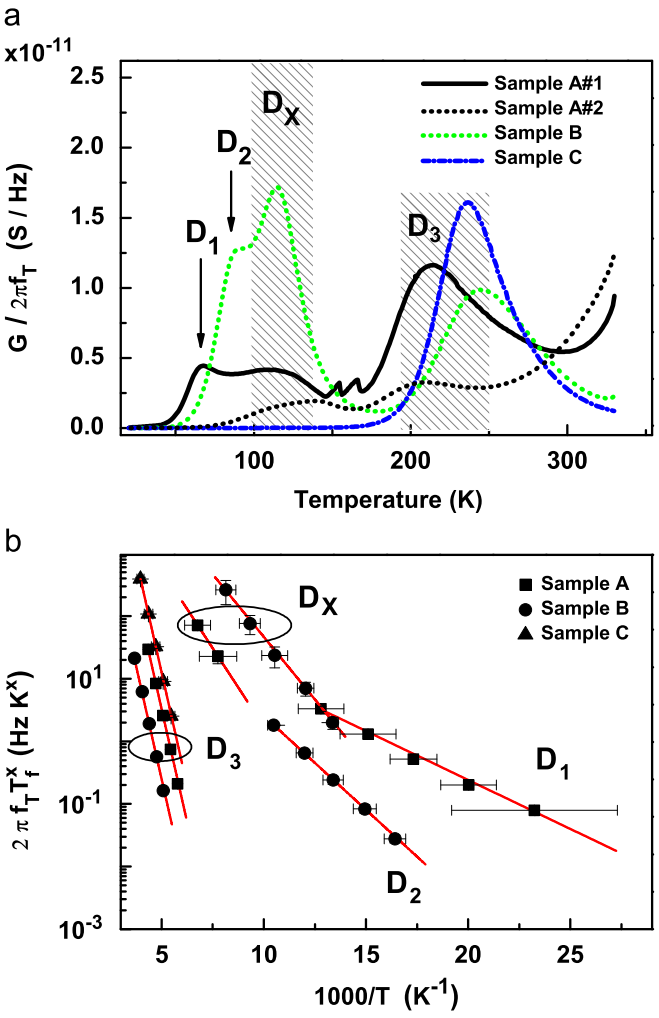

Fig. 1. (a) G/f_T temperature dependence of selected *SC*s to samples A, B and C for f_T equal to 60 kHz and at a reverse bias of −1 V. In case of sample A, different G/f_T spectra were observed depending on the *SC*s measured as shown in (a) indicating sample inhomogeneities. In (b) the Arrhenius analysis for the peaks indicated in (a) is shown. The temperature exponent x is −3 for the freeze out peaks of samples A and B corresponding to donors D_1 and D_2 respectively, while −1.5 is used in case of sample C due to the higher temperature range the freezing out on D_3 is occurring at. In all the other cases x has to be considered equal to −2.

ones generally reported for the so called E_3 defect [22]. This level is commonly attributed to oxygen vacancies [23], but recently also Fe or Ni impurities [24] as well as the second ionization level of interstitial zinc [18] have been suggested. In case of samples A and B, the D_3 level does not constitute the main level. Hence a detailed analysis according to the approach developed by Pautrat et al. [20] can be performed by using the Fermi level position (E_F) and the effective shallow donor concentration (N_{eff}) of $(1.0\pm0.3)\times10^{16}$ and $(4\pm1)\times10^{15}\,\mathrm{cm}^{-3}$ for samples A and B, respectively, as determined by *TDH* measurements [19]. In addition, the built-in voltage (V_{bi}) is needed for the analysis and a value of ~0.4 V is extracted from the *C–V* characteristics of the samples [25]. The results of the data analysis are listed in Table 2. For sample B, the value of the extrapolated (apparent) capture cross section σ_{D3} is in good agreement with the range of values reported for E_3 in the literature [11,26], that is $\sim3\text{–}6\times10^{-16}\,\mathrm{cm}^2$. However, there is experimental evidence [22] of two closely spaced levels E_3 and E_3' with a difference in energy of only ~3 meV, but with clearly different capture cross sections. Indeed, the presence of two overlapping contributions to the overall measured D_3 peak is consistent with the shift in temperature position of the D_3 peak in